MQP-BIO-DSA-4810

# ISOLATION OF VIRAL ISOLATES WITH ALTERED GROWTH PROPERTIES AND VIRULENCE

A Major Qualifying Project Report

Submitted to the Faculty of the

WORCESTER POLYTECHNIC INSTITUTE

in partial fulfillment of the requirements for the

Degree of Bachelor of Science

in

Biology and Biotechnology

by

_____
Kyle Feeley

April 30, 2009

APPROVED:

_____
Michael Brehm, Ph.D.
Division of Diabetes
Umass Medical Center
Major Advisor

_____
David Adams, Ph.D.
Biology and Biotechnology
WPI Project Advisor

# ABSTRACT

The goal of this project was to test Pichinde virus isolates for *in vitro* and *in vivo* viability, and to determine the best candidate for a new progenitor stock. This determination was made through plaque assays for the *in vitro* study, and through ICCS FACS analysis for the *in vivo* study. The results indicate that the #11 72h Pichinde isolate was the best candidate because it grew consistently to a high titer *in vitro* and produced the most pronounced immune response *in vivo*.

# TABLE OF CONTENTS

# ACKNOWLEDGEMENTS

First and foremost, I would like to extend great thanks to the Welsh lab at the University of Massachusetts Medical School in Worcester, Massachusetts, especially to Ray Welsh for welcoming me into his lab, and to Michael Brehm for advising me and being extremely helpful throughout the project. I would also like to thank Keith Daniels for all of his help and advice over the course of my eight months at UMASS. Additional thanks go out to fellow lab members Carey, Steve, Alex, Keisha, Kapil, Heather, and Mina. Finally, I must thank Dave Adams, my WPI project advisor, for his incredible help, guidance, and tireless effort in helping me see this project through from start to finish.

# BACKGROUND

## Arenavirus History

*Arenaviridae* receive their name from the Latin root Arena, meaning sand, due to the grainy appearance of ribosomes seen in virion cross-sections (Rowe et al, 1970) (**Figure-1**). These viruses are known to cause chronic infections in rodents worldwide, and often establish persistent infections during which asymptomatic animals carry and shed virus. Persistently infected rodents serve as a reservoir of virus which may be spread to humans upon contact with infected materials. Human arenavirus infections are fairly common and may be severe. Moreover, transplant patients receiving organs from donors infected with a common arenavirus, LCMV, have experienced significant morbidity and mortality (Lymphocytic…2005). The mechanisms by which *Arenaviridae* persist in rodents are complex, and their study has contributed significantly to a better understanding of immunology.

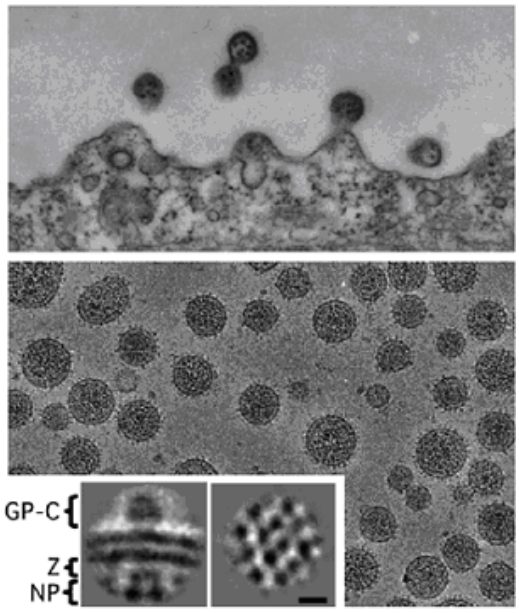


**Figure 1: Electron Microscopy of Arenaviruses.** (Field's Virology, 2006).

While studying the 1933 St. Louis encephalitis epidemic, Lillie and Armstrong were the first to isolate an arenavirus (Armstrong and Lillie, 1934). This virus, lymphocytic choriomeningitis virus (LCMV), was subsequently identified in 1935 to be the cause of human meningitis (Rivers and Scott, 1935). After this initial discovery, many other studies were conducted that determined LCMV to be a common human pathogen. Over the next forty years, other viral isolates from chronically infected rodent hosts, such as Machupo and Tacaribe were discovered to share similar morphology (Murphy et al., 1969) and serology with LCMV (Rowe et al., 1970). For those reasons, the viruses were grouped together into the *Arenaviridae* family. Currently, new arenaviruses are discovered approximately every one to three years. Though extremely similar morphologically, some of the arenaviruses cause severe symptoms in humans while others do not.

**Arenavirus Taxonomy**

The *Arenaviridae* family contains only the genus arenavirus, which includes eighteen arenavirus species, seven of which are known to be human pathogens, while eleven are not (Clegg, 2000). An important distinction made among arenaviruses is between the Old World group and the New World group, also referred to as the LCM/Lassa complex and the Tacaribe complex, respectively. While serologic assays were used to initially separate Old from New World viruses, genetic analysis has since been used to more completely investigate their interrelatedness. Nucleoprotein and glycoprotein genetic sequence analysis has made it easier to appropriately classify *Arenaviridae* (**Figure-2**). Within the New World arenaviruses, three distinct evolutionary lineages emerge. Lineage A includes Flexal, Parana, Pichinde, Pirital, Tamiami, and Whitewater Arroyo. Lineage B contains Guanarito, Junin, Machupo, Sabia,

Amapari, and Tacaribe. Lineage C is home only to two viruses, Latino and Oliveros. All four of the South American arenaviral hemorrhagic fevers are members of the B lineage, and this suggests that perhaps this phenotype was passed down by a common pathogenic ancestor.

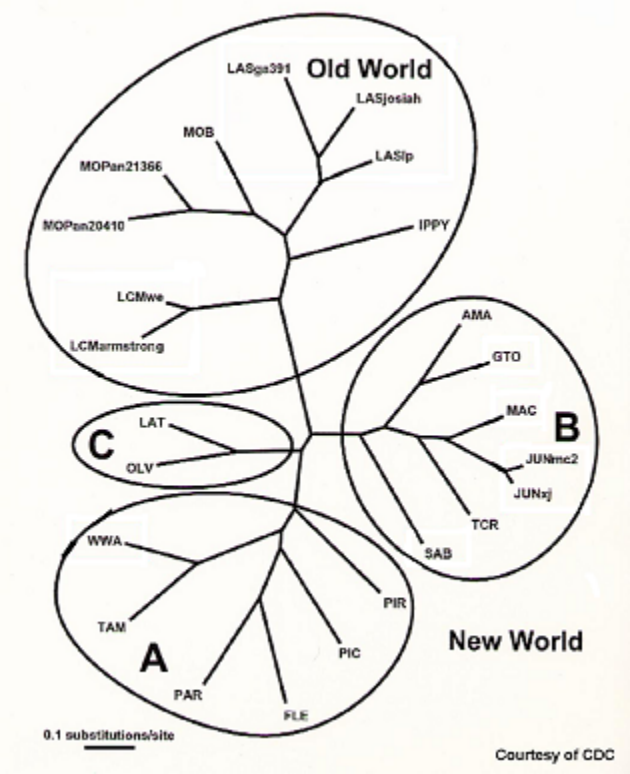


**Figure 2:** ***Arenaviridae*** **Phylogenetic Map.** (Field's Virology, 2006)

It is interesting to note that two viruses in the B lineage (Junin and Machupo) have rodent hosts of the same genus (*Calomys*), while three viruses in the A lineage (Flexal, Parana, and Pichinde) also share a common host genus (*Oryzomys*). This is evidence for co-evolution between the viruses and their host. There is no such longitudinal trend observable among Old World arenaviruses, nor are there separate and distinct evolutionary lineages. Indeed, up to a 25% nucleotide difference in the nucleoprotein gene exists between the Lassa virus strains.

**Arenavirus Structure**

Understanding viral structure is crucially important to better understanding viral function and regulation. All *Arenaviridae* are enveloped viruses that contain a segmented linear ambisense ssRNA genome. They range in size from 50 to 300 nm while averaging 110-130 nm in diameter. Tetrameric complexes of two viral glycoproteins, G1 and G2, project outward from the surface of the virion envelope (Burns and Buchmeier, 1991). As such, monoclonal antibodies against both have been developed in attempts to neutralize viral activity, though anti-G1 antibodies are more effective. Three major polypeptides are contained in the viruses, RNA transcriptase included. Arenaviruses include two nucleocapsids that are helical in shape. These nucleocapids are filamentous and form closed circles.

The two single stranded RNA segments that make up an arenavirus genome are referred to as the S and L segments, for small and large, respectively (**Figure-3**). The entire genome is approximately 10,000-11,000 nucleotides long, with 7000-7400bp making up the L segment, while the S segment is roughly 3400bp long. For a number of arenaviruses including LCVM, the complete genome has been sequenced. As shown by Auperin et al (1982), the nucleotide sequence at the 3' termini of New and Old World arenaviruses is conserved. This is important not only for its evolutionary implications, but also because the 3' termini of both the S and L RNA segments are identical at 17 of their final 19 nucleotides. Unlike many 5' ends, the 5' terminus in arenaviruses does not contain a cap. Due to the apparent circular nature of arenavirus nucleocapsids when viewed under the microscope, it is believed that the 3' and 5' ends base pair to form panhandle structures.

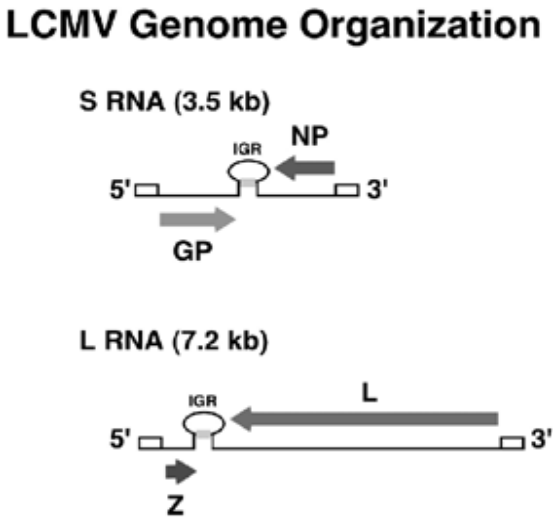


**Figure 3: Diagram of the Arenavirus Genome.** Note the existence of S and L RNA segments encoding different viral genes. The arrows denote the coding strategy. Also shown are the non-coding intergenic regions (IGR) which form 1-3 stem-loop structures that play an important role in viral entry and transcription. (Field's Virology, 2006)

The nucleoprotein and two envelope glycoproteins are both encoded by genes contained within the S RNA segment. In 1987, it was shown that GP1 and GP2 are first expressed as a precursor protein, GPC, which is then cleaved into two after translation (Buchmeier et al., 1987). Included in the L RNA segment are genes that encode the viral polymerase, or L protein, and the Z protein whose function remains unknown. The genes are oriented in an ambisense arrangement, meaning their genome contains both positive and negative sense. The ssRNA ambisense genome of arenaviruses is primarily negative-sense except for a part of the 5' ends of both fragments. The nucleoprotein gene is on the 3' end of the S RNA segment, while the polymerase gene is located at the 3' end of the L RNA segment. On the 5' ends of the S and L RNA segments reside the GPC and Z protein genes, respectively.

Between the two genes contained on each segment is an interesting intergenic region of the arenavirus genomic RNA. It was shown in 1984 that these regions, which are anywhere from 59-217 nucleotides long, form between one to three stem-loop structures in the genomic and

antigenomic sense (Auperin et al., 1984). These structures are non-coding regions of the genomic segments but they play an important role in viral entry and transcription.

**Arenaviral Proteins**

The arenavirus genome encodes four proteins: NP, GPC, Z, and L. The most important structural protein in arenavirions is the nucleoprotein (NP), which has a molecular size between 60-68 kd. The NP associates with virion RNA in an arrangement of beadlike structures. It is also the predominant protein component of their nucleocapsids. It was shown in 1986 that the NP may become phosphorylated following an acute infection, and that this new form becomes increasingly prevalent in persistent infections (Bruns et al., 1986). Once a cell has become infected, NP has been shown to localize exclusively within the cell cytoplasm. The exception to this rule is that Pichinde NP contains a degradation fragment that localizes instead within the nucleus of infected cells.

The precursor GPC protein, which is cleaved post-translationally into GP1 and GP2, is generally between 70-80 kd in size. This cleavage requires prior glycoslyation and must take place in the area surrounding the trans-Golgi network. The GP1 protein is cleaved from the amino-terminal side of the GPC while the GP2 protein is cleaved near an arginine-arginine motif which happens to be conserved in all arenaviruses except for Tacaribe. No GPC proteins remain uncleaved and this explains why both glycoproteins are found to exist in virions in equimolar amounts. The GP1 and GP2 are by no means particularly similar to one another, however. GP1 is the peripheral membrane glycoprotein and it assembles into homotetrameric complexes held together through disulfide bonding. These GP1 complexes make up the globular head of glycoprotein spikes. GP2, on the other hand, is the integral membrane glycoprotein although it

does include a membrane spanning domain. Cross-linking studies have shown that highly charged residues at the carboxyl end of GP2 molecules interact with NP in the cytosol. Similar to the homotetrameric GP1 compelxes, GP2 molecules form homotetramers and become the stalk portion of the glycoprotein spike. The GP1 and GP2 homotetramers bind one another through ionic interactions.

The L protein is the largest protein by far encoded by the arenavirus genome, with a molecular size between 180-250 kd (Lukashevich et al., 1997). The L gene site is responsible for encoding the viral polymerase, and the L protein is a component of the nucleocapsid. Alternatively, the Z protein is the smallest protein encoded by the arenavirus genome. It has a molecular size of 11 kd. As mentioned earlier, the function of the Z protein is not entirely clear, however it is believed to be a structural protein that is also a component of the nucleocapsid. Unlike NP which specifically localizes to the cytoplasm, Z protein has been shown to appear in the cytoplasm and the nucleus of LCMV-infected cells.

**Arenaviral Entry and Pathology**

The viral infectious cycle begins with entry of the virus particle into a permissive host cell. To accomplish this, arenaviruses use the GP1 part of the glycoprotein spike for initial binding to cell surface receptors. For this reason, anti-GP1 antibodies are effective against blocking viral infection. GP1 binds cellular glycoprotein alpha-dystroglycan, discovered in 1998 (Cao et al., 1998). Guanarito is an arenavirus that does not bind to alpha-dystroglycan, so it is clear that other cellular proteins may serve as arenavirus receptors. Once the arenavirus has attached to the cellular protein receptors, they enter the cell by way of a large endocytic vesicle. In 1994, the mechanism of LCMV entry into cells was published explaining how viral

nucleocapsids are delivered into host cells by pH-dependent fusion between the virion and endosomal membranes (Di Simone and Buchmeier, 1995). It is pH-dependent because the GP1 and GP2 dissociate at an acidic pH, and this triggers fusion activity.

After the nucleocapsids enter the cytoplasm, viral replication is initiated by the L protein (the viral polymerase) in a transcription method that resembles bunyaviruses (**Figure-4**). It is possible to reduce viral replication by treatment with actinomycin D, which acts to make the L protein less effective. The two RNA strands have common 3' end sequences complementary to their respective 5' ends. Occasionally, portions of the RNA will fold into stem-loop structures, and it is thought that these formations in the intergenic region have something to do with transcriptional termination by stabilizing the 3' ends. Nucleoprotein mRNA can sometimes be seen as early as two hours post-infection, while the NP itself makes its appearance sometime between 6-12 hours. It requires twice this time for any L protein to be detected, but by then the virus is present.

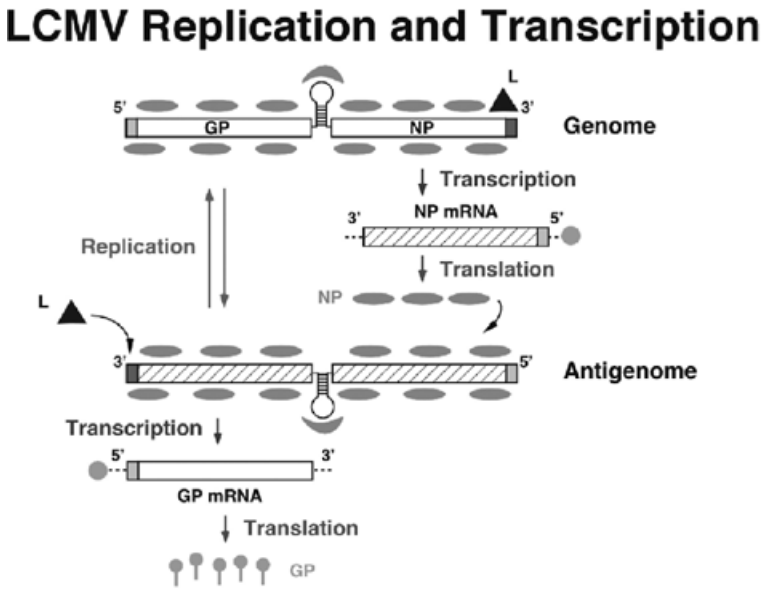


**Figure 4: Basic Arenavirus Replication and Transcription for the S Segment.** (Field's Virology, 2006)

Despite the amount of research focus directed toward arenaviruses, their precise assembly post-infection is not exactly known. The current assembly model suggests that the NP protein, L protein, and genomic RNAs combine to form nucleocapsids. Strangely, arenaviruses then arrange host-cell ribosomes into virion particles. Assuming uninhibited entry, virus assembly will proceed as a result of membrane budding, and arenaviruses are capable of easily establishing a persistent infection in rodent cells.

**Persistent Infection and Defective Interfering Particles**

A persistent infection is one in which the virus is not cleared from the host, but instead remains present in some specific cells. There are three types of persistent infection: latent, chronic, and slow. Arenavirus infections are capable of producing persistent infections in their hosts, as well as *in vitro* through a series of changes in viral gene expression. In cell culture, arenavirus infections transition from an acute phase into a persistent phase. Virus is actively being produced and replicated during the acute phase, and once this slows significantly, the virus may enter the persistent phase characterized by life-long infection. It was shown that over the time of a persistent LCMV infection, the relative amount of S RNAs becomes greater than the L RNAs (Francis and Southern, 1988). When an L cell is persistently infected, a greatly increased amount of NP is seen, while GPC, GP1, and GP2 are reduced.

A defective interfering (DI) particle is a virus without part of its genome. As a result of missing this information, DI particles or their expressed RNAs are incapable of sustaining a persistent infection by themselves, and instead require the assistance of a helper virus for co-infection. With arenaviruses, DI particles are produced during acute and persistent infections, and they interfere with viral infectivity. DI particles are actually smaller than normal infectious

virions and have a mean diameter of 55-56 nm. Among other differences from the norm, DI particles can be missing either GP1 or GP2, or they can be nonglycosylated. Additionally, the NP and GPC are abnormally sized. Interestingly, a DNA form of the LCMV S RNA has been found in the spleens of persistently infected mice (Klenerman et al., 1997).

**The Welsh Lab at UMASS Medical School**

Dr. Raymond Welsh's research pathology laboratory at UMASS Medical School (Worcester) is principally concerned with analyzing mechanisms of viral immunology and immunopathlogy. This is done through the use of mouse infection models using several viruses including vaccinia virus, herpes simplex virus, and mouse hepatitis virus. Arenaviruses such as LCMV and Pichinde are also used in the lab, among others. The Welsh lab is BSL-2 and infected mice are maintained in a BSL-2 facility. His lab showed that natural killer cells are activated during a viral infection, and are an important part of viral resistance. Taking this further, the lab is now determining exactly which viral gene products are important to NK sensitivity for a variety of viruses, and what NK functions relate to antiviral activity. Additionally, they are looking at virus-specific cytotoxic T lymphocytes induced during viral infections to examine factors that affect CTL memory, development, and maintenance.

# PROJECT PURPOSE

As stated in the Background, the Welsh lab at UMASS Medical analyzes the mechanisms of viral immunology and immunopathlogy through mouse model infections. One of the viruses analyzed is Pichinde virus (PV), an arenavirus. Recently, it became apparent that their PV experiments were not validating similar experiments conducted previously, posing a serious problem especially for longitudinal studies. It was determined that their PV progenitor stock was growing to a significantly smaller titer than their previous stock, and that this was the cause of the experimental discrepancies. The purpose of this project was to select, grow, and functionally analyze three alternative PV isolates to determine the best candidate for a new progenitor stock.

# METHODS

## Cell Lines and Media

Three different cell lines were used in this investigation. Vero cells are kidney epithelial cells derived from African green monkeys. Vero cells are frequently used as host cells for growing viruses. The cells were maintained and passed primarily in T25 flasks containing Minimum Essential Medium (MEM), 500 ml of which was supplemented with 50 mL of fetal calf serum (to 10%), 5 mL L-glutamine, 5 mL PenStrep, and 5 mL Hepes.

BHK cells are baby hamster kidney cells. BHK cells are fibroblastic and are generally used as a viral host. The cells were maintained and passed primarily in T25 flasks containing Dulbecco's Modified Eagle Media (DMEM), 500 ml of which was supplemented with 50 mL fetal calf serum (to 10%), 10 mL L-glutamine, and 5 mL PenStrep.

NCTC-929 cells are mouse immortalized liver fibroblasts. The purpose of the NCTC-929 cells was to repeat experiments previously conducted in BHK cells to determine that analogous results would be obtained using mouse cells. The cells were maintained and passed primarily in T25 flasks containing Minimum Essential Medium (MEM), 500 ml of which was supplemented with 50 mL fetal calf serum (to 10%), 5 mL L-glutamine, 5 mL PenStrep, and 5 mL Hepes.

Eagle's Minimal Essential Medium (EMEM) was used in the plaque assays. It was mixed with a recipe of 10 mL fetal calf serum, 2 mL L-glutamine, and 2 mL PenStrep.

## Virus

The Welsh lab progenitor stock for Pichinde virus lost its homogeneity over time due to its being prone to accumulating point mutations. This resulted in several emergent quasi-species.

This progenitor stock was plaqued and these quasi-species were isolated based on plaque morphology. Three of these Pichinde virus isolates (#1, #6, and #11) were selected based on differences in morphology for new progenitor stock candidate analysis. BHKs were grown in DMEM and incubated for 3 days to 70-80% confluency. A cell count was taken and total cells was determined. The following equation was used to determine how much virus should be added to one T150 of BHKs: total # of cells in the flask **x** multiplicity of infection of 0.01 / pfu/mL. Once the correct amount of virus was added for each of the three isolates, the flasks were mixed every 30 minutes for 90 minutes. After 24 hours, the T150s containing PV isolates 1, 6, or 11 had 50 mL supernatant (containing virus) taken up into separate conical tubes which were spun down for five minutes. From each isolate, seven vials were filled with 4 mL, and three additional aliquots were filled with 100 µL. These aliquots were frozen at -80C. This aliquotting process was repeated at 48 hours and once more at 72 hours. At this point, seven 4mL vials and three 100 µL aliquots were frozen for each of the three stocks at each of three time points.

**Plaque Assay**

Once virus samples were taken of each of the three stocks at three time points, a plaque assay was conducted to determine their viral titers. In order to plate the cells into 6-well plates for the plaque assay, a cell count was done. $2.5x10^5$ cells per well were prepared in 2mL of media.

In a 96-well plate, wells in the first column were filled with 200 µL of each of the nine recently frozen viral samples (e.g. #1 at 24 hours, #6 at 72 hours, etc.). A positive control was included in the final row. The remaining wells were filled with 180 µL of DMEM. The virus samples that were loaded in the first column were then serially diluted left to right across the

plate with 20 µL being taken from the first well, added to the second, mixed, and so on. The final six dilutions were added to appropriately labeled 6-well plates. The plates were tilted every 30 minutes for 90 minutes so that the virus would evenly distribute across the cells. After 90 minutes incubation, the plates were overlayed with a 50/50 mixture of EMEM and agarose. 4mL of this mixture was added to each well. The purpose of this overlay is to fix the viral plaques in place such that each plaque formation will be independent.

After 3 days incubation, the wells were stained so that the plaques would be visible and quantifiable. This staining was done by the addition of 2 mL/well of a 50/50 mixture of EMEM/agarose and 150 µL of neutral red per 10 mL total volume. This second overlay was allowed to incubate overnight, and the plaques were counted the next day.

**Intracellular Staining**

IFN-gamma producing CD8 T cells were detected using the Cytofix/Cytoperm Kit Plus (with GolgiPlug; BD PharMingen). Splenocytes ($2x10^6$ cells per culture well) were incubated with 5 µM synthetic peptide in the presence of 10 U/ml human recombinant IL-2 (BD Pharmingen) and 1 µl/ml GolgiPlug for 5 hours at 37C. Following the incubation, splenocytes were stained for cell surface markers. The samples were washed once using Staining Buffer (PBS without $Mg^{2+}$ or $Ca^{2+}$; 1% FCS, 0.09% Sodium Azide) with 200 µl/well, and centrifuged for 5 minutes at 1200 rpm. FC receptors were blocked using 2.4G2 antibody for 5 minutes at 4°C in 100 µl of staining buffer. 100 µl of staining buffer was added in another wash, which was centrifuged for 5 minutes at 1200 rpm. The cells were stained for surface antigens using appropriate antibodies in 100 µl of staining buffer for 20 minutes at 4°C. Cells were washed twice with staining buffer. Samples were then fixed and permeabilized with Cytofix/Cytoperm

solution for 20 minutes at 4C. Cells were washed twice in 1X Perm/Wash solution (dilute 10X stock in $dH_2O$). They were then resuspended in 100 µl of Perm/Wash solution containing anti IFN-gamma (clone XMG1.2; BD Pharmingen). The samples were incubated for 25 minutes at 4°C, washed twice with 1X Perm/Wash, washed with staining buffer, and put into a final volume of 300µl staining buffer for analysis. The samples were analyzed using a BD LSR II Analyzer (BD Biosciences) and CellQuest Software (BD Biosciences).

**Tetramer FACS Staining**

Splenocytes ($2x10^6$) were added per well for staining followed by the addition of 100 µl of FACS buffer to each well. Samples were centrifuged and decanted. FC block was diluted 1:100 into FACS buffer, and 100 µl of this was added to each well to block non-specific staining. Cells were incubated for 5 minutes at 4°C, and then centrifuged for five minutes and decanted. 100 µl of FACS buffer was added, and then cells were costained with indicated peptide-loaded tetramer and anti-CD8 clone, after which cells were incubated for 45 minues at 4°C. After washing twice with FACS buffer, samples were stained for intracellular IFN-gamma as described above.

**Mice and *In Vivo* Infections**

C57BL/6 mice were purchased from Jackson Laboratories (Bar Harbor, ME) at 5-6 weeks of age. Mice were infected with $10^7$ pfu of PV through IP injection. After 3 days, spleens and fatty pads were harvested and manually ground with a drill press. A plaque assay, as described previously, was conducted on the spleens and fatty pads in order to determine viral load. After 8 days, spleens were harvested and intracellular stain and tetramer stain protocols

were conducted as described previously. All experiments were done in compliance with institutional guidelines as approved by the Institutional Animal Care and Use Committee of the University of Massachusetts Medical School (Worcester, MA).

# RESULTS

The goal of this project was to investigate the viability and functionality of several Pichinde virus isolates (#1, #6, #11) previously prepared in our laboratory to determine the best potential candidate for developing a new progenitor stock. The current lab stocks had proven unreliable relative to earlier lab experiments, and it would be imprudent to proceed with rodent infections without first proving that the viruses were viable and can replicate in a host organism. In order to accomplish this, viral growth was measured and compared *in vitro* and *in vivo*.

### *In Vitro* Plaque Assays

The three previously prepared Pichinde isolates were freshly grown in BHK cell culture and harvested at 24h, and 48h time points. These harvested aliquots were serially diluted in 6 well plates, and the $10^6$ dilutions of each were added onto a single 6-well plate. After mixing with agarose, the plates were incubated overnight, then stained and the plaques were counted (**Table I**). Sample #1 taken at 24 hrs produced the highest titer of virus, and the rest of the samples were approximately equal and slightly lower. However, this was far too little information to make a determination that #1 was the best stock candidate, as it dropped significantly in titer between samples taken at 24h and 48h. The main purpose for this plaque assay was to observe relative plaque morphology. The #11 plaques were the most consistently clear and evenly sized while the #6 plaques were rather varied and fuzzy. The #1 isolate produced a mixture of sharp and fuzzy plaques without much size variation.

**Table I. Plaque Assay Count for Pichinde Viral Isolates PV #1, 6, 11 at 24h and 48h Plated on Vero Cells**

| Sample | Incubation Time | Number of Plaques in the $10^6$ Dilution | Titer |
|---|---|---|---|
| Control | | 5 | $5x10^6$ |
| 1 | 24 Hr | 91 | $9.1x10^7$ |
| 1 | 48 Hr | 51 | $5.1x10^7$ |
| 6 | 24 Hr | 52 | $5.2x10^7$ |
| 6 | 48 Hr | 68 | $6.8x10^7$ |
| 11 | 24 Hr | 55 | $5.5x10^7$ |
| 11 | 48 Hr | 41 | $4.1x10^7$ |

In order to get a determination of the stock titers, the same time points were plaqued once more in vero cells, this time plaques were quantitated at both $10^6$ and $10^7$ dilutions (**Table II**). As before, the $10^6$ dilution saw double digit plaque formation, and stock #1 taken at 24 hrs as the highest titer, but the $10^7$ dilution likely better represents the viral titers, and several stocks gave titers equivalent to #1 at 24 hr. Interestingly, the number of plaques are noticeably lower in the $10^6$ dilution the second time around. This is not cause for concern, however, as the log order is the same, and the decrease was uniform which would suggest a possible procedural difference. The purpose for this plaque assay was to get working stocks of each viral isolate with a known titer.

**Table II. Plaque Assay Count for Pichinde Viral Isolates PV #1, #6, and #11 at 24h and 48h Plated on Vero Cells**

| Sample | Incubation Time | Number of Plaques in the | | Titer |
|---|---|---|---|---|
| | | $10^6$ Dilution | $10^7$ Dilution | |
| Control | | ND | ND | ND |
| 1 | 24 Hr | 33 | 5 | $5x10^7$ |
| 1 | 48 Hr | 27 | 4 | $4x10^7$ |
| 6 | 24 Hr | 13 | 1 | $1x10^7$ |
| 6 | 48 Hr | 21 | 5 | $5x10^7$ |
| 11 | 24 Hr | 20 | 3 | $3x10^7$ |
| 11 | 48 Hr | 18 | 5 | $5x10^7$ |

Now that working stocks of each viral isolate had been generated, the next step was to characterize their growth kinetics relative to one another. For this, the 72h time point was included in the next plaque assay (**Table III**).

**Table III. Plaque Assay Count for Pichinde Viral Isolates PV #1, #6, and #11 at 24h, 48h, and 72h Plated on Vero Cells to Observe Growth Kinetics**

| Sample | Incubation Time | Number of Plaques in the | | | | | Titer |
|---|---|---|---|---|---|---|---|
| | | $10^4$ Dilution | $10^5$ Dilution | $10^6$ Dilution | $10^7$ Dilution | $10^8$ Dilution | |
| Control | | ** | 56 | 7 | 0 | 0 | $7x10^6$ |
| 1 | 24 Hr | ** | ** | 20 | 2 | 0 | $2x10^7$ |
| 1 | 48 Hr | **** | ** | 99 | 24 | 0 | $2x10^8$ |
| 1 | 72 Hr | **** | ** | 33 | 10 | 0 | $1x10^8$ |
| 6 | 24 Hr | ** | 29 | 2 | 0 | 0 | $2x10^6$ |
| 6 | 48 Hr | **** | ** | 28 | 0 | 0 | $2x10^7$ |
| 6 | 72 Hr | **** | **** | ** | 15 | 0 | $1x10^8$ |
| 11 | 24 Hr | **** | ** | 17 | 3 | 0 | $3x10^7$ |
| 11 | 48 Hr | **** | ** | 45 | 7 | 0 | $7x10^7$ |
| 11 | 72 Hr | **** | ** | ** | 19 | 2 | $2x10^8$ |

*(****: full lawn, ***: >200 estimated, **: 100-200 estimated)*

The addition of the 72h samples in this plaque broadens the scope significantly and presents a new standout candidate: #11 72h. This isolate reached the largest maximum titer and shows a continuous rate of growth. This sample grew out to $2x10^8$ which was matched only by #1 48h. Curiously, #1 24h was not the frontrunner it was once. In addition to quantifying viral titer by counting plaques, it is important to note plaque appearance. Across the board, the #11 plaques were the most consistently uniform. The #1 plaques were fairly uniform, and the #6 plaques were highly variable and fuzzy.

Now that it had been shown that the viral strains were growing considerably well in BHK cells and that there were emerging excellent progenitor candidates, the next step was to perform the same experiment in mouse cells. It is entirely possible that the isolates could grow well in one type of cell and not in another. NCTC-929 cells are mouse immortalized liver fibroblasts. Similarly strong growth in the NCTC-929 cells would be enough evidence to initiate *in vivo* experimentation. The three isolates at each of the three time points were added to NCTC-929 cells (**Table IV**). In addition, another plaque assay was done simultaneously from isolates added to BHK cells to serve as a control.

**Table IV. Plaque Assay Count for Pichinde Viral Isolates PV #1, #6, and #11 at 24h, 48h, and 72h to Compare NCTC-929 Growth to BHK Control.**

| | | Number of Plaques in the | | | | | | | | | | | |
|---|---|---|---|---|---|---|---|---|---|---|---|---|---|
| | | $10^4$ Dilution | | $10^5$ Dilution | | $10^6$ Dilution | | $10^7$ Dilution | | $10^8$ Dilution | | Titer | |
| Sample | Incubation Time | BHK | NCTC-929 | BHK | NCTC-929 | BHK | NCTC-929 | BHK | NCTC-929 | BHK | NCTC-929 | BHK | NCTC 929 |
| Control | | | *** | | ** | | 29 | | 2 | | 0 | | $2x10^7$ |
| 1 | 24 Hr | 62 | 3 | 12 | 0 | 0 | 0 | 0 | 0 | 0 | 0 | $1.2x10^6$ | $3x10^4$ |
| 1 | 48 Hr | *** | 30 | ** | 1 | 72 | 0 | 8 | 0 | 0 | 0 | $8x10^7$ | $1x10^5$ |
| 1 | 72 Hr | *** | ** | ** | 79 | 82 | 5 | 9 | 1 | 1 | 0 | $1x10^8$ | $1x10^7$ |
| 6 | 24 Hr | * | * | 15 | 12 | 1 | 0 | 0 | 0 | 0 | 0 | $1x10^6$ | 1.2x10 |
| 6 | 48 Hr | *** | ** | ** | 31 | 42 | 3 | 5 | 0 | 1 | 0 | $1x10^8$ | $3x10^6$ |
| 6 | 72 Hr | *** | *** | ** | 112 | 61 | 18 | 10 | 2 | 0 | 0 | $1x10^8$ | $2x10^7$ |
| 11 | 24 Hr | ** | 52 | 44 | 3 | 5 | 0 | 0 | 0 | 0 | 0 | $5x10^6$ | $3x10^5$ |
| 11 | 48 Hr | *** | ** | ** | 59 | 23 | 14 | 0 | 0 | 0 | 0 | $2x10^7$ | 1.4x10 |
| 11 | 72 Hr | *** | *** | ** | ** | 31 | 30 | 4 | 4 | 0 | 0 | $4x10^7$ | $4x10^7$ |

It is apparent from the table that each of the Pichinde isolates did indeed grow successfully in the NCTC-929 cells. Once again, the standout is #11 72h, this time followed closely by the other two 72h samples. It is interesting to note that none of the 24h samples grew to high titers in this experiment. Also, the BHK plaques produced a reduced titer across the board as compared to the previous BHK plaque so it is important to compare the NCTC-929 growth to the BHK growth in this experiment and not to previous BHK growth. With this in mind, this was the final positive evidence necessary to greenlight *in vivo* analysis.

### *In Vivo* Activity of the Viral Stocks

In order to determine whether the viral isolates that had been shown to grow well *in vitro* were capable of similar growth *in vivo*, C57 mice were infected with each isolate and the plaque titer determined for the spleens and fat pads. As described in the Methods, groups of four C57BL/6 (age 5-6 weeks) mice were infected with $10^7$ pfu of each PV isolate through IP

injection (samples 1-4 infected with PV isolate #1, samples 5-8 infected with #6, samples 9-12 infected with #11). After 3 days, four of the six mice infected with each isolate had their spleen and fatty pads harvested and manually ground with a drill press. A plaque assay (described previously) was conducted on the spleens and fatty pads (**Table V**) to determine viral load.

**Table V. Plaque Assay for Spleens of Infected C57 Mice.**
Viral Load Determination for Pichinde Viral Isolates PV #1, #6, and #11 at 24h, 48h, and 72h 3 Days Post-Infection.

| | Number of Plaques in the | | | | | | | | | |
|---|---|---|---|---|---|---|---|---|---|---|
| | $10^1$ Dilution | | $10^2$ Dilution | | $10^3$ Dilution | | $10^4$ Dilution | | $10^5$ Dilution | |
| Sample | Spleen | Fat Pads | Spleen | Fat Pads | Spleen | Fat Pads | Spleen | Fat Pads | Spleen | Fat Pads |
| 1 | 0 | 14 | 0 | 3 | 0 | 0 | 0 | 0 | 0 | 0 |
| 2 | 4 | 11 | 8 | 1 | 2 | 0 | 0 | 0 | 0 | 0 |
| 3 | 0 | 22 | 1 | 5 | 0 | 1 | 0 | 0 | 0 | 0 |
| 4 | 0 | 20 | 0 | 4 | 0 | 0 | 0 | 0 | 0 | 0 |
| 5 | 0 | 14 | 0 | 6 | 0 | 1 | 0 | 0 | 0 | 0 |
| 6 | 0 | 31 | 4 | 4 | 0 | 1 | 0 | 0 | 0 | 0 |
| 7 | 0 | 17 | 0 | 3 | 0 | 1 | 0 | 0 | 0 | 0 |
| 8 | 0 | 25 | 1 | 4 | 0 | 1 | 0 | 0 | 0 | 0 |
| 9 | ** | **** | ** | ** | 60 | 25 | 8 | 3 | 0 | 0 |
| 10 | ** | **** | * | *** | 12 | 27 | 0 | 1 | 1 | 0 |
| 11 | ** | **** | ** | *** | 49 | 50 | 3 | 6 | 0 | 3 |
| 12 | ** | **** | ** | *** | 30 | 22 | 0 | 3 | 0 | 0 |
| control | **** | **** | *** | 54 | 10 | | | | | |
| | $10^3$ Dilution | $10^4$ Dilution | $10^5$ Dilution | $10^6$ Dilution | $10^7$ Dilution | | | | | |

*(Samples 1-4 were infected with PV isolate #1, 5-8 infected with #6, 9-12 infected with #11)*

It is clear that the four samples infected with viral isolate #11 (samples 9-12) show significantly higher viral titers *in vivo* in both the spleen and fat pads. This is further evidence in favor of #11 being the best progenitor candidate. The samples infected with #1 and #6 show evidence of virus in the fat pads out to the $10^3$ dilution, but very little virus is seen in the spleens.

It is important to observe plaque morphology and uniformity. Observing plaque morphologies is a preliminary way of determining homogeneity of the viral isolate. High variance would suggest possible contamination or mutation. Relative plaque size is also related to the amount of virus. Hazy or turbid plaques are indicative of lysogenic reproduction and clear plaques indicate lytic reproduction. Photographs were taken of PV isolate #11 (sample 9 showing the highest viral load) for plaques from spleen (**Figure-5**) and fat pads (**Figure-6**).

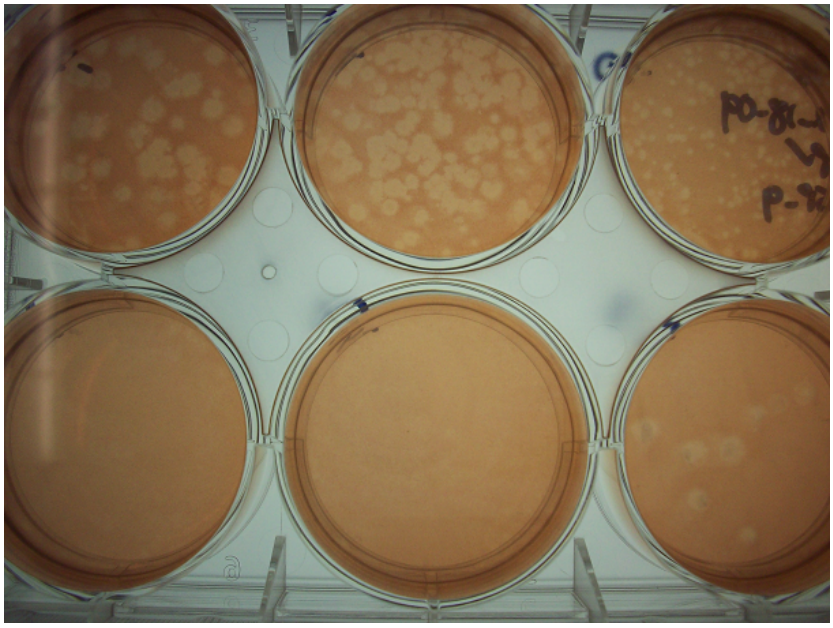

**Figure 5: Photograph of the Spleen Plaques Induced by PV Isolate #11, Sample 9.**

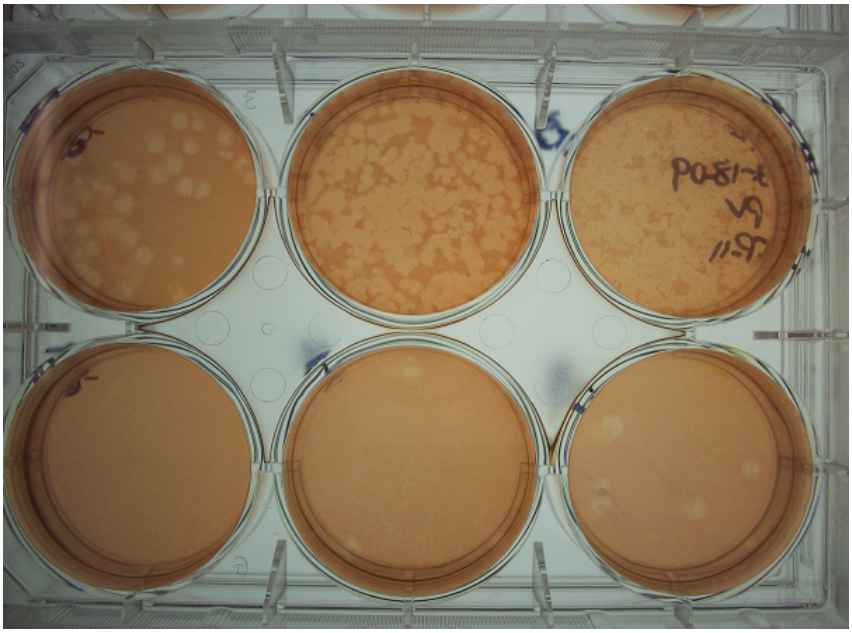

**Figure 6: Photograph of the Fat Pad Plaques Induced by PV Isolate #11, Sample 9.**

In both cases, fairly consistent plaque morphology was observed. At lower dilutions, there is an apparent size disparity between some of the plaques, but they become increasingly more consistent at higher dilutions. From this experiment it can be concluded that in spite of infecting the mice with the same viral titers (as assayed *in vitro*), *in vivo* the #11 PV isolate was found in much higher quantities in spleen and fat pads than the other isolates three days following infection.

FACS analysis was performed on splenocytes to quantify IFNγ-producing CD8 T cells, whose levels are a measure of cellular immune activity (**Figure-7**). Mice were infected in the same manner as described before with equal titers of the three viral isolates. Two mice were infected with #1 72h, two were infected with #6 72h, and three were infected with #11 72h (as this latter was the isolate of most interest). In addition, two naïve mice were used as negative controls in this experiment. After 8 days, the spleens were harvested and the splenocytes were stained for cell surface markers, and analyzed by FACS as described in the Methods.

The naïve mice should not return evidence of an immune response because they were never infected with virus. The first two rows show this to be true. The unstimulated column acts as another control; there should not be a noticeable response in this column because no peptides antibodies were added. With the exception of the mouse #3 infected with #11 72h, this holds true. The anti-CD3 monoclonal antibody was used here because it serves as a polyclonal stimulation for T cells. CD3 antigens are part of the T cell receptor complex and, upon engagement, will activate the T cell. NP38-45 is a short peptide derived from the Pichinde nucleoprotein that is the dominant target for Pichinde-induced T cell responses. Like CD3, NP38 positive for IFNγ production indicates immune system activity. NP205-212 is another short peptide derived from the Pichinde nucleoprotein. The CD8 T cell response to the NP205 epitope is generally very weak.

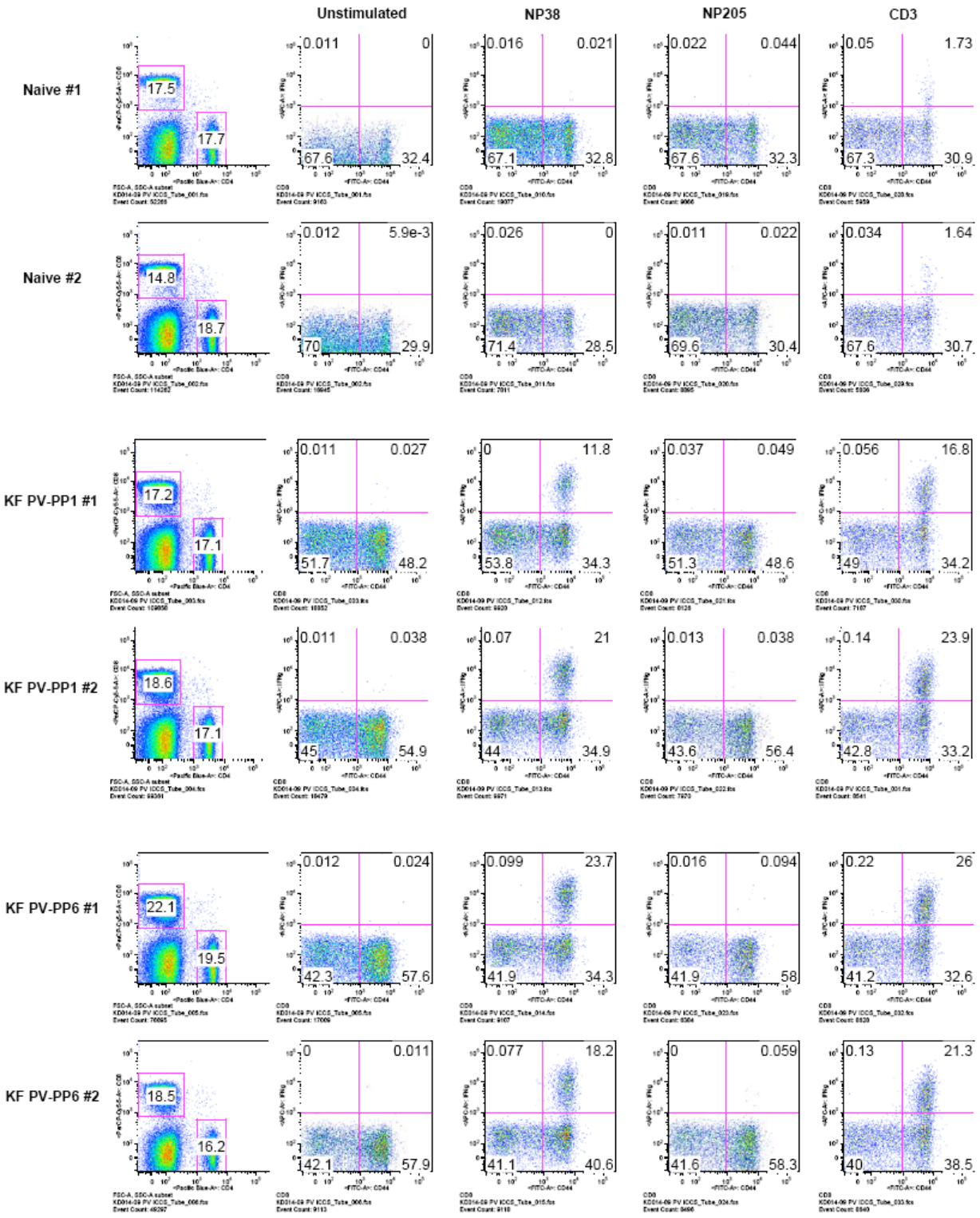
Unstimulated
NP38
NP205
CD3
Naive #1
17.5
17.7
0.011
0
67.6
32.4
0.016
0.021
67.1
32.8
0.022
0.044
67.6
32.3
0.05
1.73
67.3
30.9
Naive #2
14.8
18.7
0.012
5.9e-3
70
29.9
0.026
0
71.4
28.5
0.011
0.022
69.6
30.4
0.034
1.64
67.6
30.7
KF PV-PP1 #1
17.2
17.1
0.011
0.027
51.7
48.2
0
11.8
53.8
34.3
0.037
0.049
51.3
48.6
0.056
16.8
49
34.2
KF PV-PP1 #2
18.6
17.1
0.011
0.038
45
54.9
0.07
21
44
34.9
0.013
0.038
43.6
56.4
0.14
23.9
42.8
33.2
KF PV-PP6 #1
22.1
19.5
0.012
0.024
42.3
57.6
0.099
23.7
41.9
34.3
0.016
0.094
41.9
58
0.22
26
41.2
32.6
KF PV-PP6 #2
18.5
16.2
0
0.011
42.1
57.9
0.077
18.2
41.1
40.6
0
0.059
41.6
58.3
0.13
21.3
40
38.5

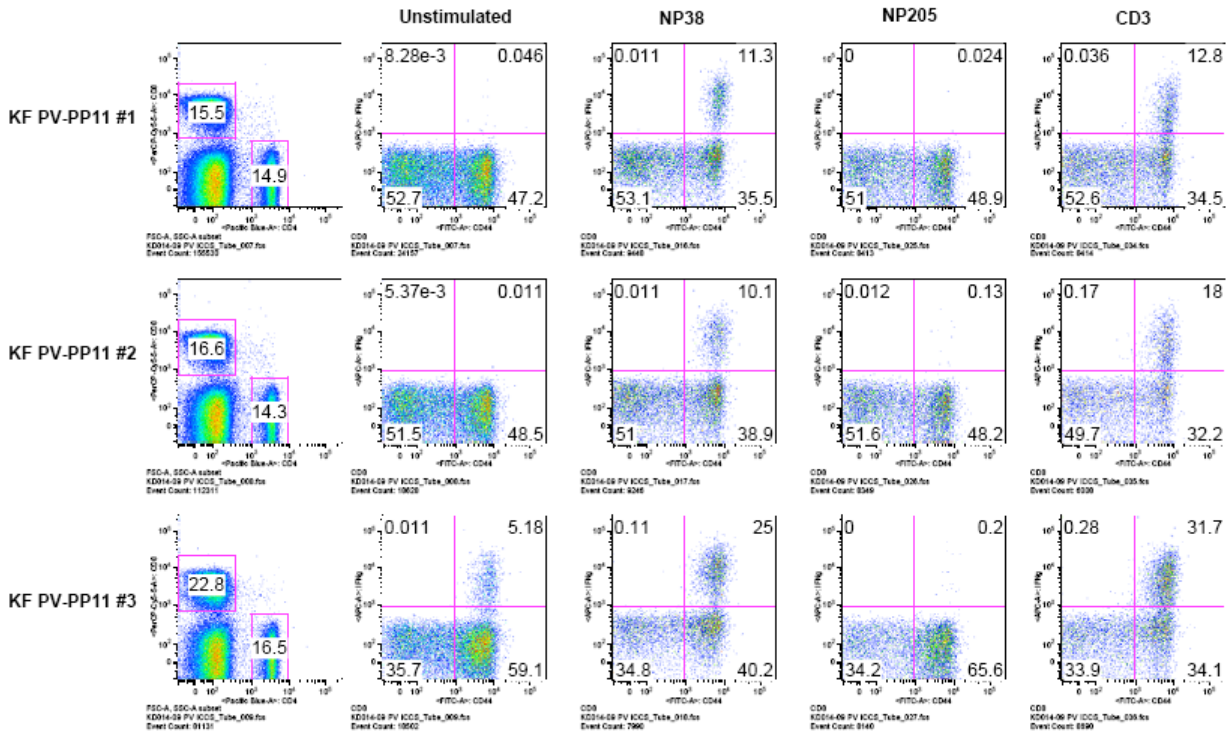


**Figure 7: ICCS FACS Analysis of Mouse Splenocytes**. The Y axis is IFNγ and the X axis is CD44. CD3 antigens were screened as a T-cell activation marker. NP38 is a PV nucleoprotein-derived peptide that plays a dominant role in Pichinde infection immune responses. NP205 is another nucleoprotein-derived peptide that is subdominant.

The naïve mice produced no response to the NP38, NP205, or CD3 antibodies. The #1 isolate produced a noticeable response to NP38 and CD3, although it reaches 11.8% in mouse #1 and was 21% for mouse #2, despite receiving the same amount of the same virus, such differences are not uncommon. The #6 isolate shows a greater immune response in that the maximum NP38 is higher (23.7%) and it has a higher average. While the #11 isolate produced the largest NP38 percentage of all (25%), its average is decidedly lower. None of the mice showed any significant amount of NP205, which was not especially alarming because the CD8 T cell response to NP205 is subdominant. The purpose of quantifying the percent of active splenocytes is to determine virulence. Considering all three isolates were injected into mice at

the same number of plaque forming units, the one to induce the strongest immune response is the most virulent.

A tetramer stain was conducted with the same goal in mind as the ICCS (**Figure-8**) to quantify the percentage of splenocytes active in the PV immune response. Biotinylated streptavidin MHC tetramers were used to quantify the percentage of antigen-specific T cells. The tetramer works by fluorescently labeling any T cell that expresses T cell receptors specific to the peptide. Only NP38 and NP205 tetramers were analyzed. Cells were gated on CD44 as an activation marker, and then again on the two tetramers. The percentages of NP38 tetramer positive cells are relatively low for each viral isolate, and surprisingly low for the #11 isolate. NP205 detection is virtually nonexistent which is not surprising as it usually shows weak response. Consistent with the ICCS results, viral isolate #11 underperformed relative to expectations based on its high titers *in vitro*.

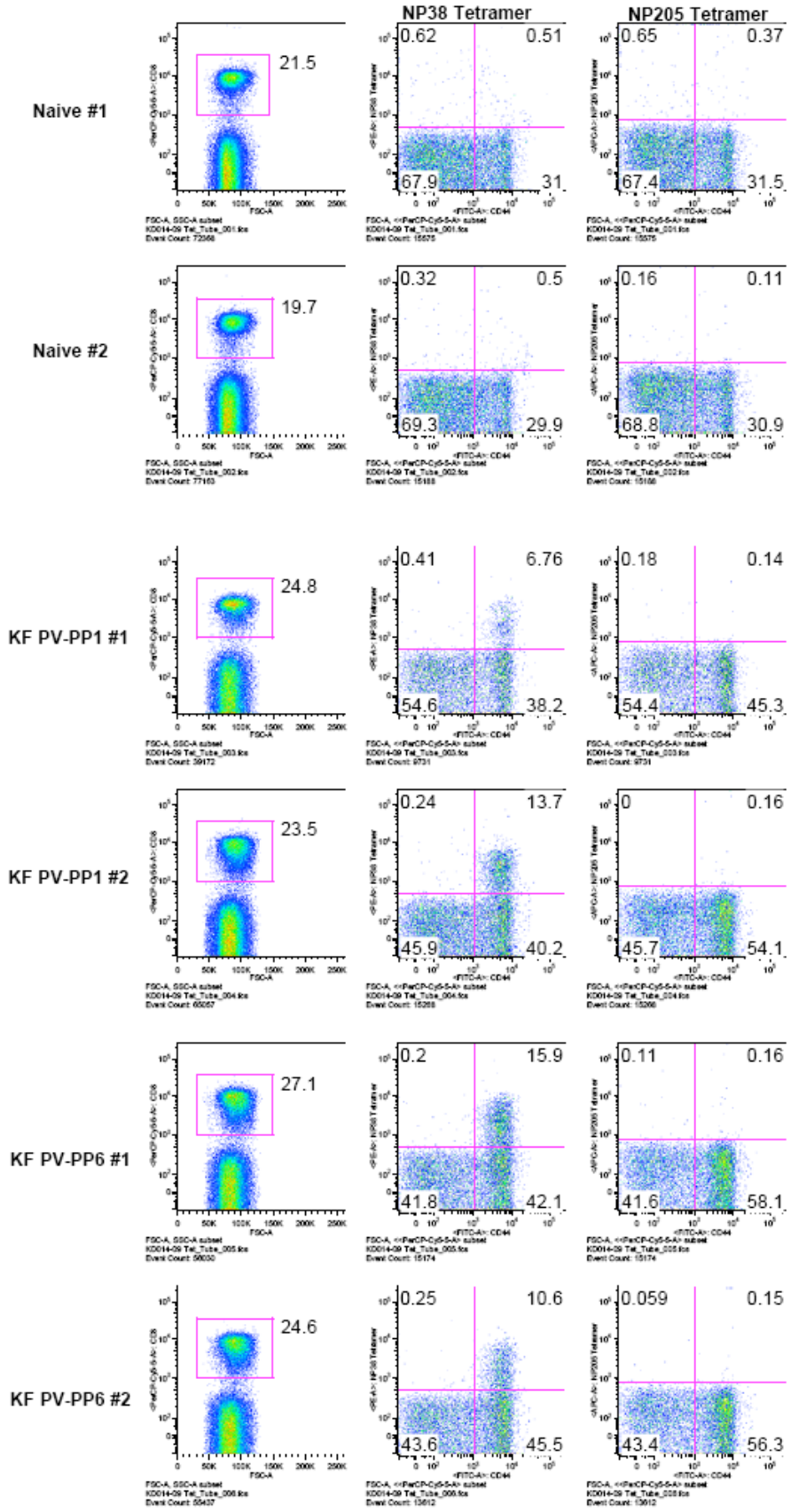
NP38 Tetramer
NP205 Tetramer
Naive #1
21.5
0.62
0.51
67.9
31
0.65
0.37
67.4
31.5
Naive #2
19.7
0.32
0.5
69.3
29.9
0.16
0.11
68.8
30.9
KF PV-PP1 #1
24.8
0.41
6.76
54.6
38.2
0.18
0.14
54.4
45.3
KF PV-PP1 #2
23.5
0.24
13.7
45.9
40.2
0
0.16
45.7
54.1
KF PV-PP6 #1
27.1
0.2
15.9
41.8
42.1
0.11
0.16
41.6
58.1
KF PV-PP6 #2
24.6
0.25
10.6
43.6
45.5
0.059
0.15
43.4
56.3

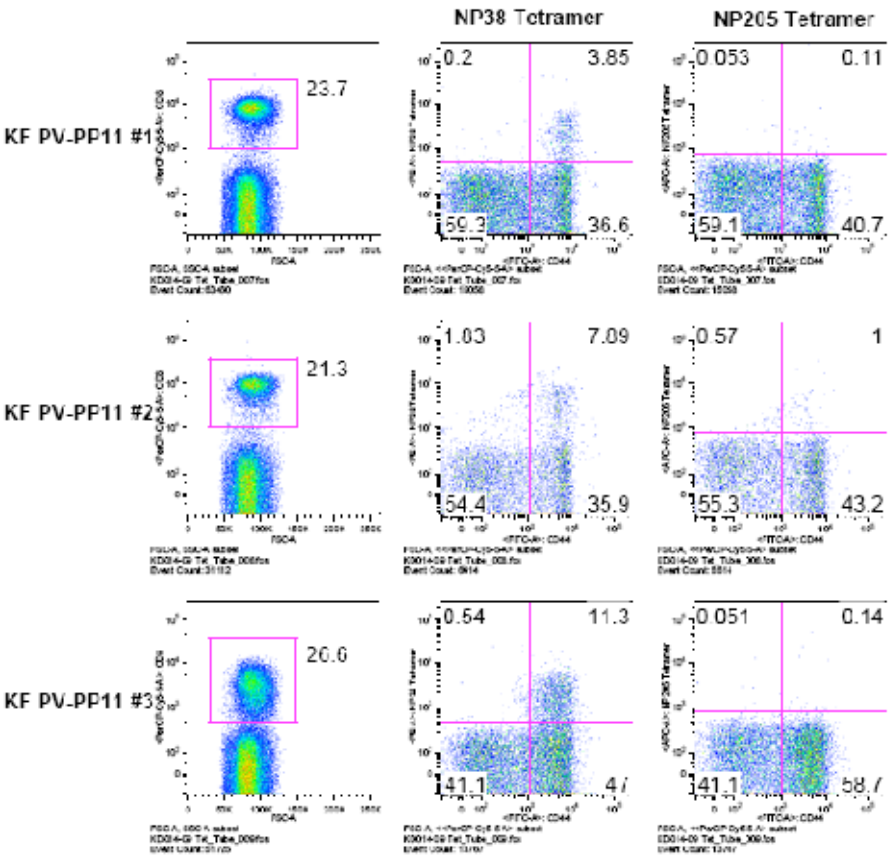


**Figure 8: Tetramer FACS Analysis of Infected Mice.** The Y axis for the middle and last column is NP38 tetramer and NP205 tetramer, respectively. The X axis is CD44 activation marker.

# DISCUSSION

Pichinde virus is highly susceptible to point mutations which, when accumulated over time, may dramatically alter the homogeneity of a viral stock. Such a situation occurred to the Pichinde progenitor stock in the Welsh lab at UMASS Medical School (Worcester). To initiate development of another stock, viral isolates were examined *in vitro,* and then *in vivo* in mice for growth kinetics, characteristics, and virulence.

Initially, the *in vitro* analysis indicated viral isolate #11 72h as a promising candidate. In the BHK plaque assay, it reached the highest titer ($2x10^8$) and showed a continuous growth rate. In addition to a strong titer, the #11 isolate in general had the most uniform looking plaque formations, sharp and similarly sized. The #1 48h isolate and the #6 72h isolate also grew to high titers in BHK cells. However *in vitro* titers determined on BHK cells is not always a good indicator of potency, as growth in BHK does not necessarily translate to growth in mice. To resolve this, another *in vitro* plaque assay was performed using NCTC-929 mouse liver cells. Here, the #11 72h isolate was the best candidate, reaching the highest titer ($4x10^7$). What was more important with respect to the second round of experiments was it showed the virus could grow in mouse cells.

Further evidence of the apparent superiority of the #11 isolate was found *in vivo*. Splenocytes and fat pads harvested from C57 mice three days after infection showed that isolate #11 produced significantly higher titers than the other two isolates. Indeed, isolates #1 and #6 were barely detectable in the spleens, while #11 grew to $10^4$ consistently. All evidence using

mouse cells or mice thus far had shown that the #11 isolate, particularly #11 72h, was the clear choice for creating a new progenitor Pichinde virus stock.

The FACS analysis experiments cast some doubts on the obviousness of #11 as the choice isolate. Infection with #11 produced the largest measured NP38 response (25%) in the ICCS experiment, but the average NP38 response was 15%. In contrast, the #6 isolate produced consistently high NP38 and CD3 responses. It is important to remember, however, that the #6 isolate had a variable and fuzzy spleen and fat pad plaque morphology, and that #11 is still likely the superior isolate. #6 was shown to induce the largest response when stained for NP38 tetramer as well. The disparity is not particularly great, though, and it certainly does not definitively show either isolate to be better.

Major difficulties with the project were rare, but one in particular stands out. In both the ICCS and tetramer results, there are no noticeable responses to NP205. NP205, like NP38, is a peptide derived from the viral nucleoprotein that is active in immune response. It was expected that some NP205 antigen would be present in the infected spleen cells, but none was found in any of the mice. Although NP205 is subdominant and CD8 T cell response to it is generally very weak, the hope was that at least one of the isolates might induce a noticeable response. It is possible that the NP205 antibodies used are no longer intact. This is not necessarily the case, though, as the weak response was consistent among the viral isolates and the original virus.

In the future, another member in the Welsh lab is going to purify the #11 72h isolate. To do this, the virus will be added to T150 flasks containing BHK cells and then incubated for four days. After incubation, the supernatants from the flasks containing virus will be harvested into 50mL tubes and centrifuged to clear cellullar debris. The supernatants will then be layered onto 20-60% sucrose gradients, and following centrifugation, the purified virus should rest between

the 20% and 60% sucrose layers. This progenitor stock will be used in future Welsh lab PV experiments.

# BIBLIOGRAPHY


Armstrong C, Lillie RD (1934) Experimental lymphocytic choriomeningitis of monkeys and mice produced by a virus encountered in studies of the 1933 St. Louis encephalitis epidemic. *Public Health Reports* **49**: 1019–1027.

Auperin DD, Compans RW, Bishop DH (1982) Nucleotide sequence conservation at the 3' termini of the virion RNA species of New World and Old World arenaviruses. *Virology* **121(1):** 200–203.

Auperin DD, Galinski M, Bishop DH (1984) The sequences of the N protein gene and intergenic region of the S RNA of pichinde arenavirus. *Virology*. **134(1)**: 208–219.

Bruns M, Zeller W, Rohdewohld H, Lehmann-Grube F (1986) Lymphocytic choriomeningitis virus. IX. Properties of the nucleocapsid. *Virology*. **151(1)**: 77–85.

Buchermier MJ, Southern PJ, Parekh BS, Woodell MK & Oldstone MBA (1987) Site specific antibodies define a cleavage site conserved among arenavirus GP-C glycoproteins. *Journal of Virology* **61**: 982-985.

Burns J W, Buchmeier M J (1991) Protein-protein interactions in lymphocytic choriomeningitis virus. *Virology* **183(2)**: 620-629.

Cao W, Henry MD, Borrow P, et al. (1998) Identification of alpha-dystroglycan as a receptor for lymphocytic choriomeningitis virus and Lassa fever virus. *Science*. **282(5396)**: 2079–2081.

Clegg JCS (1992) Current progress towards vaccines for arenavirus-caused diseases. *Vaccine* **10**: 89–95.

Di Simone C, Buchmeier MJ (1995) Kinetics and pH dependence of acid-induced structural changes in the lymphocytic choriomeningitis virus glycoprotein complex. *Virology*. **209(1)**: 3–9 .

Francis SJ, Southern PJ (1988) Deleted Viral RNAs and Lymphocytic Choriomeningitis Virus Persistence *in vitro*. *Journal of General Virology*. **69**: 1893-1902.

Klenerman P, Hengartner H, Zinkernagel RM (1997) A non-retroviral RNA virus persists in DNA form. *Nature*. **390**: 298–301.

Lukashevich et al. (1997) The Lassa fever virus L gene: nucleotide sequence, comparison, and precipitation of a predicted 250 kDa protein with monospecific antiserum. *Journal of General Virology*. **78**: 547-551.

"Lymphocytic Choriomeningitis Virus Infection in Organ Transplant Recipients," Morbidity and Mortality Weekly Report. 2005. **54(21)**: 537-539.

Murphy FA, Webb PA, Johnson KM, Whitfield SG (1969) Morphological comparison of Machupo with lymphocytic choriomeningitis virus: basis for a new taxonomic group. *Journal of Virology* **4(4)**: 535–541.

Rivers TM, Scott TFM (1935) Meningitis in man caused by a filterable virus. *Science* **81**: 439–440.

Rowe WP, Murphy FA, Bergold GH, et al. (1970) Arenoviruses: proposed name for a newly defined virus group. *Journal of Virology* **5(5)**: 651–652.

Rowe WP, Pugh WE, Webb PA, Peters CJ (1970) Serological relationship of the Tacaribe complex of viruses to lymphocytic choriomeningitis virus. *Journal of Virology* **5(3)**: 289–292.